

AD-A275 972

ENTATION PAGE

Form Approved
OBM No. 0704-0188



to average 1 hour per response, including the time for reviewing instructions, searching existing data sources, gathering and on of information. Send comments regarding this burden or any other aspect of this collection of information, including suggestions to reduce the burden, to the Office of Management and Budget, Paperwork Project Director (0704-0188), Washington, DC 20503.

1. Agency Use Only (Leave blank).		2. Report Date. April 1993	3. Report Type and Dates Covered. Final - Journal Article	
4. Title and Subtitle. Reverberation Fluctuations from a Smooth Seafloor			5. Funding Numbers. Program Element No. 0602435N Project No. RJ035 Task No. V11 Accession No. DN294409 Work Unit No. 12401B	
6. Author(s). Steve Stanic and Edgar G. Kennedy			8. Performing Organization Report Number. JA 243:055:91	
7. Performing Organization Name(s) and Address(es). Naval Research Laboratory Ocean Acoustics Branch Stennis Space Center, MS 39529-5004			10. Sponsoring/Monitoring Agency Report Number. JA 243:055:91	
9. Sponsoring/Monitoring Agency Name(s) and Address(es). Naval Research Laboratory Center for Environmental Acoustics Stennis Space Center, MS 39529-5004			11. Supplementary Notes. Published in IEEE.	
12a. Distribution/Availability Statement. Approved for public release; distribution is unlimited.			12b. Distribution Code.	
13. Abstract (Maximum 200 words). High-frequency shallow-water reverberation statistics were measured from a smooth, sandy, featureless seafloor. The reverberation statistics are presented as a function of source frequency (20-180 kHz), grazing angle (30°, 20°, 9.5°) and source beamwidths (1.2°-2.75°). Generally, the reverberation statistics did not follow a Rayleigh fading model. The model dependence of the reverberation statistics exhibited a complex behavior that ranged from near Gaussian to beyond log-normal. The results show that small changes in the source frequency, grazing angles, and beamwidths caused large variations in the model dependence of the reverberation statistics.				
14. Subject Terms. High frequency, acoustic scattering, backscattering, forward scattering, sound transmission, underwater acoustics			15. Number of Pages. 5	
17. Security Classification of Report. Unclassified			18. Security Classification of This Page. Unclassified	
19. Security Classification of Abstract. Unclassified			20. Limitation of Abstract. SAR	
16. Price Code.			Availability Codes Dist Avail and/or Special A-1 20	

DTIC
ELECTE
FEB 22 1994
S E D

94-05401



DTIC QUALITY INSPECTED 8

NSN 7540-01-280-5500

94 2 18 00 9

Standard Form 298 (Rev. 2-89)
Prescribed by ANSI Std. Z39-18
298-102

Reverberation Fluctuations from a Smooth Seafloor

Steve Stanic and Edgar G. Kennedy

Abstract—High-frequency shallow-water reverberation statistics were measured from a smooth, sandy, featureless seafloor. The reverberation statistics are presented as a function of source frequency (20–180 kHz), grazing angle (30°, 20°, 9.5°) and source beamwidths (1.2°–2.75°). Generally, the reverberation statistics did not follow a Rayleigh fading model. The model dependence of the reverberation statistics exhibited a complex behavior that ranged from near Gaussian to beyond log-normal. The results show that small changes in the source frequency, grazing angles, and beamwidths caused large variations in the model dependence of the reverberation statistics.

I. INTRODUCTION

HIGH-RESOLUTION rough-surface reverberation measurements have shown that in general, Rayleigh fading models do not provide an adequate description of rough-surface clutter statistics. Rough surface reverberation measurements made using high-resolution radars and sonars have measured scattered envelope amplitude distributions that are described by Gaussian, Rayleigh, log-normal, Weibull or other more complex probability density functions (PDF) [1]–[9]. High-resolution sonars have also been used to measure seafloor reverberation [10], [11]. *et al.* Boehme [12] and Stanic *et al.* [13] have shown that sea floor reverberation statistics also show significant departures from Rayleigh fading models. In all cases, the scattering statistics have been shown to be highly dependent on sonar frequency and beamwidth. McDaniel has related Boehme's and Chotiros' [11], [12] results at 30 kHz to the measured bottom micro-roughness spectrum [14]. Stanton [15], [16] has shown that the shape of the PDF can provide a measure of the relative levels of coherent and incoherent scattering. Stanton has also related the PDF shapes to estimates of bottom roughness, correlation lengths, and bottom microstructure. These results have all assumed that the seafloor returns were not contaminated by scattering from subsurface volume scatterers. Alexandrou *et al.* [17] have compared reverberation PDF's generated by point scatterer model simulations with sea beam reverberation data. This comparison lead to identifying acoustic signatures to be used in seafloor classification.

This paper presents high-resolution seafloor reverberation statistics as a function of frequency (20–180kHz), grazing angle (30°, 20°, 9.5°) or equivalent range intervals (lengths of insonified bottom area at the –3-dB points), and system

Manuscript received August 1, 1991; revised December 1, 1992. This work was supported by the Office of Naval Technology, Program Element 62435N, and by the Office of Naval Research, Program Element 61153N, through the NOARL Defense Research Sciences Program. This paper is NRL Contribution 243:055:91.

The authors are with the Naval Research Laboratory, Stennis Space Center, MS 39529-5004.

IEEE Log Number 9207375.

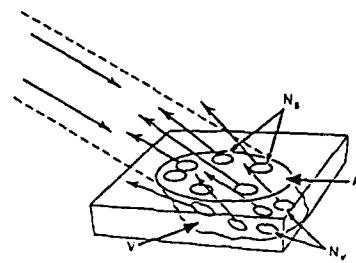


Fig. 1. Schematic of insonified seafloor with N_s and N_v surface and volume scatterers.

beamwidths (1.2°–2.75°). The results are compared to various theoretical RDF models and to PDF's measured for a coarse shell bottom during the Jacksonville experiments [13].

Fig. 1 shows acoustic energy incident on a surface area A that contains N_s surface scatters. In addition, the acoustic energy that penetrates into the sea floor is scattered by a variety of individual volume scatterers N_v . For the monostatic backscattering case, the signal at the output of a receiving sonar sensor is given by

$$V_i = B_i V_{i0} \exp [j(\omega\tau - 2kr_i + \theta_i)]$$

where V_{i0} is the backscattering amplitude, θ_i is the scattering phase of the signal scattered from the i th scatterer, r_i is the range between the sonar receiving sensors and the i th scatterer, $k = 2\pi/\lambda$ is the acoustic wave number, and λ is the acoustic wave length, ω is the angular frequency, τ is time, and B_i is a system constant that accounts for system calibrations, propagation losses, and other system related factors. If the scatterers are independent, then the total reverberation field due to the N_s and N_v scatterers can be expressed as

$$V = \sum_{i=1}^N B_{i0} \exp^{j\Phi_i}$$

where $\Phi_i = \omega\tau - 2kr_i + \theta_i$ and N is the total number of scatterers.

This total reverberation field will in general fluctuate around some mean value. It is the PDF of these fluctuations that identify the noise models against which target detection algorithms must operate. For example, a processor optimized for Rayleigh noise would perform poorly when operating against a non-Rayleigh noise. The probability of false alarm (PFA), defined as one minus the cumulative distribution function, can also be used to characterize reverberation fluctuations. The PFA is a more sensitive measure of the differences in the tails of various PDF's than the cumulative distribution function.

The PFA for a Rayleigh PDF is given by [18]

$$\text{PFA}(y) = \exp(-10^{y/10}).$$

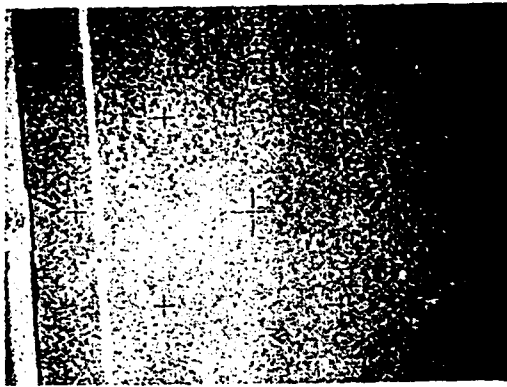


Fig. 2. Bottom photograph showing the smooth featureless seafloor.

For a log normal distribution the PFA is given by [19]

$$PFA(y) = \int_y^{\infty} \exp \frac{-((y - \beta)/\sigma)^2}{\sigma\sqrt{2\pi}} dy$$

where β is calculated from

$$1 - \int_{-\infty}^{\infty} 10^{y/10} \frac{\exp[-((y - \beta)/\sigma)^2]}{\sigma\sqrt{2\pi}} dy$$

σ is defined as the standard deviation.

The PFA for a Gaussian PDF can be expressed as [20]

$$PFA(y) = \text{erfc} \left[\frac{y - m}{\sigma} \right]$$

where m is the signal mean, σ the standard deviation, and erfc the error function.

II. EXPERIMENTAL MEASUREMENTS

A series of high-resolution bottom reverberation measurements were made in an area 19 miles south of Panama City, FL. The seafloor in this area was smooth, with only small shell fragments spatially distributed in the sand. Fig. 2 is a photograph of the sea floor. A detailed experimental description of the measurement area is given in Stanic *et al.* [21].

Bottom reverberation measurements were made using NRL's stable acoustic measurement system [22]. The acoustic measurements were made using a pair of nonlinear parametric sources and a two-dimensional 12-hydrophone spatial array. Source beamwidth as a function of frequency for the 250-kHz and 450-kHz sources operating parametrically are shown in Table I. Data from the receiving hydrophone located at the center of the receiving array were processed using a high-speed computer automated measurement and control system (CAMAC). The data were complex base banded to 5 kHz, digitized at 20 kHz and recorded on a high-speed parallel transfer disk. Individual reverberation envelopes were calculated and the results recorded on optical disks. At each grazing angle, the source frequency was varied between 20 and 180 kHz, thus, the areas insonified by the 450-kHz source always contained the areas insonified by the 250-kHz source.

TABLE I
SOURCE BEAMWIDTHS AS A FUNCTION OF FREQUENCY

	Frequency kHz	Beamwidth (-3 dB)
250-kHz source	20	2.5°
	40	2.0°
	60	1.5°
	90/NB (Narrowbeam)	1.2°
450-kHz source	90/WB (Widebeam)	2.75°
	110	2.2°
	150	2.0°
	180	2.0°

TABLE II
HORIZONTAL RANGE INTERVALS AS A FUNCTION OF GRAZING ANGLE AND WIDEST SOURCE BEAMWIDTH (450-KHZ SOURCE)

Grazing angle	Frequency kHz	-3 dB beamwidth	Horizontal range interval number	Horizontal range interval length (m)
30°	90	2.75°	I	12.4-13.9
20°	90	2.75°	II	19.4-22.5
9.5°	90	2.75°	III	39.5-53.2

Table II shows the horizontal range intervals for the widest source beamwidth (450 kHz) at each grazing angle.

For each experimental configuration, reverberation data were taken for about 3 minutes using 5-ms long continuous wave (cw) pulses transmitted at 1-s intervals. Since the reverberation data were taken using sonars mounted on a stable platform, any ping-to-ping envelope amplitude variations were caused by fluctuations in the structure of the water column. These fluctuations caused changes in the size and position of the insonified areas. This introduced a random component into the reverberation envelopes that increased with range.

III. AMPLITUDE STATISTICS

The data taken at each experiment configuration were tested for stationarity using the Mann-Whitney test [23]. This test is a nonparametric test that can be used to determine if data points form part of a locally stationary sequence on a ping-to-ping basis. For each experimental configuration 3000 samples were used to calculate the PDF's of the reverberation amplitude envelopes. For a two tailed test at $\alpha = 0.05$, i.e., 95% confidence level, the test statistic (Z_n) must be less than 1.96 in order for the data points to be considered as coming from the same population and density function. Table III shows the first 20 test statistics at selected frequencies and range intervals. At these and all other frequencies and range intervals, Z_n was less than 1.96.

The reverberation distribution functions were normalized so as to have a mean of one and plotted as the probability of false alarms (PFA). These results are compared to theoretical Rayleigh and log-normal distributions with standard deviations of 5.57 dB [24] and to a Gaussian distribution with a mean of zero and a standard deviation of one. Fig. 3 shows PFA curves as a function of frequency (180, 150, 110, and 90

TABLE III
MANN-WHITNEY TEST STATISTICS (Z_n) FOR
SELECTED FREQUENCIES AND RANGE INTERVALS

Frequency 180 kHz Range Interval I	Frequency 90 kHz/WB Range Interval II
$Z_1 = 0.19647$	$Z_1 = 0.03524$
$Z_2 = 0.09996$	$Z_2 = 0.10571$
$Z_3 = 0.03792$	$Z_3 = 0.11746$
$Z_4 = 0.09307$	$Z_4 = 0.19968$
$Z_5 = 0.34124$	$Z_5 = 0.01175$
$Z_6 = 0.05170$	$Z_6 = 0.29365$
$Z_7 = 0.45844$	$Z_7 = 0.10571$
$Z_8 = 0.25852$	$Z_8 = 0.03524$
$Z_9 = 0.01034$	$Z_9 = 0.04698$
$Z_{10} = 0.32056$	$Z_{10} = 0.08222$
$Z_{11} = 0.53427$	$Z_{11} = 0.11746$
$Z_{12} = 0.22405$	$Z_{12} = 0.09397$
$Z_{13} = 0.15511$	$Z_{13} = 0.03524$
$Z_{14} = 0.51359$	$Z_{14} = 0.14095$
$Z_{15} = 0.49291$	$Z_{15} = 0.04698$
$Z_{16} = 0.27920$	$Z_{16} = 0.17619$
$Z_{17} = 0.52381$	$Z_{17} = 0.04698$
$Z_{18} = 0.74109$	$Z_{18} = 0.02349$
$Z_{19} = 0.72730$	$Z_{19} = 0.22318$

Frequency 60 kHz Range Interval I	Frequency 20 kHz Range Interval III
$Z_1 = 0.17274$	$Z_1 = 0.50212$
$Z_2 = 0.60459$	$Z_2 = 0.48013$
$Z_3 = 0.19865$	$Z_3 = 0.11362$
$Z_4 = 0.06910$	$Z_4 = 0.35307$
$Z_5 = 0.38003$	$Z_5 = 0.26022$
$Z_6 = 0.12092$	$Z_6 = 0.11362$
$Z_7 = 0.30229$	$Z_7 = 0.20891$
$Z_8 = 0.50095$	$Z_8 = 0.00611$
$Z_9 = 0.33654$	$Z_9 = 0.12583$
$Z_{10} = 0.10364$	$Z_{10} = 0.47524$
$Z_{11} = 0.01727$	$Z_{11} = 0.22113$
$Z_{12} = 0.00864$	$Z_{12} = 0.04276$
$Z_{13} = 0.06910$	$Z_{13} = 0.08185$
$Z_{14} = 0.16410$	$Z_{14} = 0.17470$
$Z_{15} = 0.00000$	$Z_{15} = 0.44836$
$Z_{16} = 0.25047$	$Z_{16} = 0.40194$
$Z_{17} = 0.04318$	$Z_{17} = 0.23334$
$Z_{18} = 0.06046$	$Z_{18} = 0.12339$
$Z_{19} = 0.11228$	$Z_{19} = 0.20402$

kHz/WB) and range interval for the data taken using the 450-kHz source. The data at 180, 150, 110, and 90 kHz/WB and at all range intervals showed significant departures from Gaussian, Rayleigh, and log-normal models. At range interval III the data at 150, 110, and 90 kHz/WB tended to follow a PFA other than log-normal. At range interval II the 180 and 150 kHz data tended more toward Gaussian than did the same data at range interval I. Only at 90 kHz/WB did the data show a sequential model dependence with increasing range interval. The PFA curves at 90 kHz/NB, 60, 40, and 20 kHz are shown in Fig. 4. These data were taken using the 250-kHz parametric source. The data at 90 kHz/NB and range interval

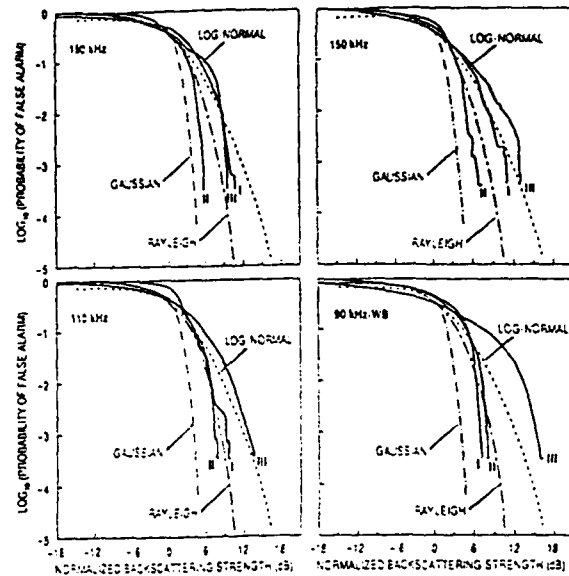


Fig. 3. Probability of false alarms as a function of frequency and range intervals.

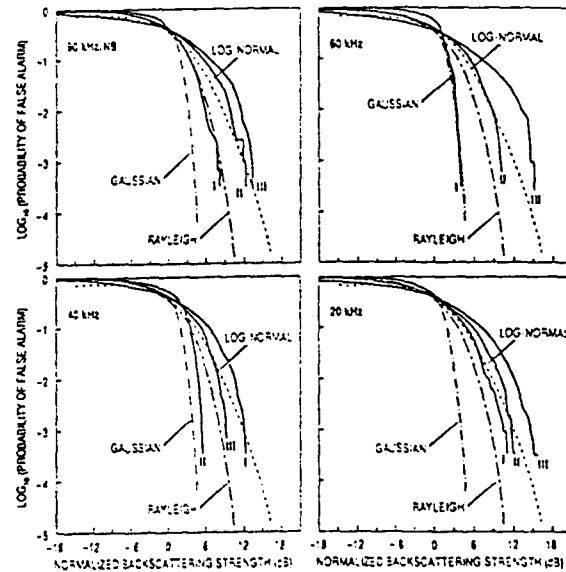


Fig. 4. Probability of false alarms as a function of frequency and range intervals.

II tended to follow a Rayleigh model. At range intervals I and III the 90-kHz/NB data tended to follow PFAs that were characteristic of high-ground clutter. At 60, 40, and 20 kHz the data at all range intervals showed significant departure from all chosen theoretical PFA models. Only at 60 kHz and for probability of false alarms less than -1 did the data tend to follow a Gaussian curve. These results are also summarized in Table IV.

IV. BEAMWIDTH DEPENDENCE

Fig. 5 shows the PFA dependence on system beamwidth and range intervals at 90 kHz. The data were taken using the 450-kHz and 250-kHz source transmitting parametrically at 90 kHz with a beamwidth of 2.75° (WB) and 1.2° (NB) respectively. At range interval I, the steepest grazing angle,

TABLE IV

PFA MODEL TENDENCY AS A FUNCTION OF RANGE INTERVAL AND FREQUENCY

Range Interval I						
Model	Gaussian	Between Gaussian and Rayleigh	Rayleigh	Between Rayleigh and log-normal	log-normal	Greater than log-normal
Freq-kHz						
180				X		
150				X		
110				X		
90WB		X				
90NB					X	
60	X					
40						X
20				X		

Range Interval II						
Model	Gaussian	Between Gaussian and Rayleigh	Rayleigh	Between Rayleigh and log-normal	log-normal	Greater than log-normal
Freq-kHz						
180		X				
150		X				
110		X				
90WB				X		
90NB			X			
60				X		
40		X				
20						X

Range Interval III						
Model	Gaussian	Between Gaussian and Rayleigh	Rayleigh	Between Rayleigh and log-normal	log-normal	Greater than log-normal
Freq-kHz						
180		X				
150						X
110						X
90WB						X
90NB						X
60						X
40				X		
20						X

the 90 kHz (WB) data tend to lie between a Gaussian and log-normal curve, depending on the value of PFA. The NB data tended to follow a model other than a high-clutter log-normal model. At range interval II, both the WB and NB data tended to converge on the Rayleigh curve. At range interval III, both the WB and NB data showed significant departures from a log-normal curve. These results are also summarized in Table V.

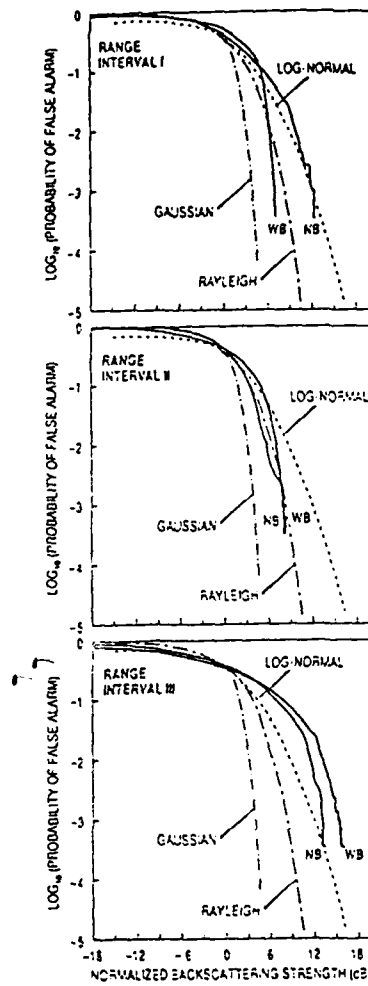


Fig. 5. Probability of false alarms as a function of system beamwidth of 90 kHz.

TABLE V
PFA MODEL TENDENCY AS A FUNCTION OF RANGES INTERVAL AND SOURCE BEAMWIDTH AT 90 kHz

Model	Gaussian	Between Gaussian and Rayleigh	Rayleigh	Between Rayleigh and log-normal	log-normal	Greater than log-normal
Range Int.						
I	WB				NB	
II			NB	WB		
IV						NB, WB

V. DISCUSSION

The results presented in this paper show that reverberation fluctuations measured from a sandy sea floor exhibit large PFA variations. Even so, this area was in general considered smooth (non-resolvable topographical features). Changes in the size and location of the insonified area resulted in large variations in the model dependence of the bottom reverberation statistics as a function of frequency, range interval, and system beamwidth.

The reverberation statistics measured from this sandy area had different model, frequency, and range interval dependen-

cies than the reverberation statistics measured from the shell covered area off Jacksonville, FL [13]. At the Jacksonville site, data taken at 180, 150, and 110 kHz and at range interval I tended to lie between Gaussian and Rayleigh PFAs. The Panama City data taken at the same frequencies and similar range intervals had a different model dependence. At frequencies at 180, 150, and 110 kHz, the model dependence at range interval II was between Gaussian and Rayleigh.

A comparison of the Panama City and Jacksonville PFA's at 90, 60, 40, and 20 kHz showed that the Panama City data was spread between Gaussian and log-normal, while the Jacksonville data was in general spread between Rayleigh and PFA's that were characteristics of a clutter environment that was higher than that of a log normal PFA. For the Panama City data, only one PFA curve tended to follow a Rayleigh model: 90 kHz/NB at range interval II.

For the Panama City, Jacksonville, and all other reported bottom reverberation data, it is assumed that the reverberation was caused by scatterers located on the sea floor surface. Recently, Boyle and Chotiros [25] have shown that even at angles below critical a considerable amount of acoustic energy can penetrate the sea floor sediment. The critical angle for the Jacksonville data was 26° . Thus, the reverberation statistics must be a function of both surface and volume scatterer distributions. These scatterers can have a large range of sizes, some distributed randomly and others distributed in all types of uneven and patchy configurations. In addition, their scattering facets can be oriented at all angles with respect to the maximum response axes of the sonar system. Because of this complexity, no current theory can completely describe the effects of the various scatterer distributions on the model dependence of the reverberation statistics. The authors will attempt to address some of these questions with data taken during a series of scattering experiments scheduled for the Gulf of Mexico in August 1993.

ACKNOWLEDGMENT

The authors would like to thank R. H. Love and R. W. Farwell of NRL and N. P. Chotiros of ARL/UT for their helpful comments.

REFERENCES

- [1] G. V. Trunk, "Radar properties of non-Rayleigh sea clutter," *IEEE Trans. Aerospace Electron. Syst.*, vol. AES-8, pp. 196-204, 1972.
- [2] G. V. Trunk and S. F. George, "Detection of targets in non-Gaussian sea clutter," *IEEE Trans. Aerospace Electron. Syst.*, vol. AES-6, pp. 620-628, 1970.
- [3] J. I. Marcum, "A statistical theory of targets detected by pulsed radar," *IRE Trans. Inform. Theory*, vol. IT-6, pp. 59-144, 1960.
- [4] P. Swerling, "Probability detection for fluctuating targets," *IRE Trans. Inform. Theory*, vol. IT-6, pp. 269-308, 1960.
- [5] F. T. Ulaby, T. F. Haddock, and R. T. Austin, "Fluctuation statistics of millimeter-wave scattering from distributed targets," *IEEE Trans. Geosci. Remote Sensing*, vol. 26, pp. 268-281, 1988.
- [6] F. T. Ulaby, F. K. Kouyate, B. Brisco, and T. H. Lee Williams, "Technical information in SAR images," *IEEE Trans. Geosci. Remote Sensing*, vol. 24, pp. 235-245, 1986.
- [7] P. N. Mikhalevsky, "Characteristics of cw signals propagating under the ice in the Arctic," *J. Acoust. Soc. Am.*, vol. 70, pp. 1717-1727, 1981.
- [8] —, "Envelope statistics of partially saturated processes," *J. Acoust. Soc. Am.*, vol. 72, pp. 151-158, 1982.
- [9] G. B. Goldstein, "False-alarm regulation in lognormal and Weibull clutter," *IEEE Trans. Aerospace Electron. Syst.*, vol. AES-9, pp. 84-92, 1973.
- [10] D. Marandino, "Low-frequency reverberation measurements with an activated towed array: Scattering strengths and statistics," *SACLANT Center Rep. SR-112*, 1987.
- [11] N. P. Chotiros, H. Boehme, T. G. Goldsberry, S. P. Pitt, R. A. Lamb, A. L. Garcia, and R. A. Altenburg, "Acoustic backscatter at low grazing angles from the ocean bottom. Part II—Statistical characteristics of bottom backscatter at a shallow water site," *J. Acoust. Soc. Am.*, vol. 77, pp. 975-982, 1985.
- [12] H. Boehme and N. P. Chotiros, "Acoustic backscattering at low grazing angles from the ocean bottom," *J. Acoust. Soc. Am.*, vol. 84, pp. 1018-1029, 1988.
- [13] S. Stanic and E. Kennedy, "Fluctuations of high-frequency shallow-water seafloor reverberation," *J. Acoust. Soc. Am.*, vol. 91, pp. 1967-1973, 1992.
- [14] S. T. McDaniel, "Seafloor reverberation fluctuations," *J. Acoust. Soc. Am.*, vol. 88, pp. 1530-1535, 1990.
- [15] T. K. Stanton, "Echo fluctuations from the rough sea floor: Predictions based on acoustically measured micro-relief properties," *J. Acoust. Soc. Am.*, vol. 78, pp. 715-721, 1985.
- [16] T. K. Stanton, "Sonar estimates of seafloor micro-roughness," *J. Acoust. Soc. Am.*, vol. 75, pp. 809-818, 1984.
- [17] D. Alexandrou, C. de Moustier, and G. Haralbus, "Evaluation and verification of bottom acoustic reverberation statistics predicted by the point scattering model," *J. Acoust. Soc. Am.*, vol. 91, pp. 1403-1413, 1992.
- [18] R. V. Waterhouse, "Statistical properties of reverberant sound fields," *J. Acoust. Soc. Am.*, vol. 43, pp. 1436-1441, 1968.
- [19] M. L. Boas, *Mathematical Methods in the Physical Sciences*. New York: Wiley, 1983.
- [20] C. W. Helstrom, *Probability and Stochastic Processes for Engineers*. New York: MacMillan, 1988.
- [21] S. Stanic, K. B. Briggs, P. Fleischer, R. I. Ray, and W. B. Sawyer, "Shallow-water high-frequency bottom scattering off Panama City, Florida," *J. Acoust. Soc. Am.*, vol. 83, pp. 2134-2144, 1988.
- [22] S. Stanic, P. Fleischer, K. B. Briggs, M. P. Richardson, and B. Eckstein, "High-frequency acoustic bottom scattering experiments, Part I—Instrumentation and methods," *NOARL Rep. 78*, 1987.
- [23] J. H. Zar, *Biostatistical Analysis*. Englewood Cliffs, NJ: Prentice-Hall, 1987.
- [24] G. V. Frisk, "Intensity statistics for long-range acoustic propagation in the ocean," *J. Acoust. Soc. Am.*, vol. 64, pp. 257-259, 1978.
- [25] F. A. Boyle and H. P. Chotiros, "Experimental detection of a slow wave in sediment at shallow grazing angles," *ARL-TR-91-14*, May 1991.



Steve Stanic received the B.S. degree in mathematics and physics from Sir George Williams University, Montreal, in 1967, the M.S. degree in aerospace engineering in 1970, and the Ph.D. degree in physics from The Pennsylvania State University, University Park, in 1976.

From 1977 to 1980 he was a research associate at the Applied Research Laboratory of The Pennsylvania State University. He is currently a Research Physicist for the Naval Research Laboratory at the Stennis Space Center in Mississippi. From 1987 to 1988 he was a Visiting Scholar in the Department of Electrical Engineering and Computer Science at the University of California, San Diego.



Edgar T. Kennedy received the Associate of Arts degree in pre-engineering from Yuba College, Yuba City, AL, in 1970.

From 1971 to 1974 he worked for Raytheon Services Company and Computer Science Corporation developing life cycle analysis models for the Safeguard Missile Command. From 1974 to 1989 he worked as a senior system software analyst for Control Data Corporation in charge of real-time operating systems development for the Kwagalein Missile test range. He is currently Head, Computer Resources Group, Ocean Acoustics Branch of the Ocean Acoustics Division of the Naval Research Laboratory.